THE ASTROPHYSICAL JOURNAL, 475:L21–L24, 1997 January 20

MOLECULAR GAS AND INFRARED EMISSION IN HCG 31 AND HCG 92 (STEPHAN'S QUINTET) AND TIDAL INTERACTIONS IN COMPACT GROUP ENVIRONMENT

M. S. YUN[1]
California Institute of Technology, Pasadena, CA 91125

AND

L. VERDES-MONTENEGRO, A. DEL OLMO, AND J. PEREA
Instituto de Astrofisica de Andalucia, CSIC, Apdo. 3004, 18080 Granada, Spain
Received 1996 August 9; accepted 1996 October 30

ABSTRACT

We present the interferometric measurements of 2.6 mm CO ($J = 1 \rightarrow 0$) emission ($\theta_{FWHM} \sim 5''$) and the analysis of *IRAS* HIRES images of two Hickson compact groups HCG 31 and HCG 92 ("Stephan's Quintet"). The far-infrared (FIR) emission is concentrated to a single region in HCG 31 while it is clearly extended and peaks near the group center in HCG 92. CO emission is weak in HCG 31, and the brightest peak occurs in the overlap region between the galaxies A and C. CO emission is detected only in galaxy C (NGC 7319) in HCG 92, and the distribution is highly asymmetric. No CO emission is detected in the interacting pair HCG 92 B and D (NGC 7318 A and B). Gas stripping and star formation by continuous tidal disruptions in compact group environment are discussed as possible explanations for the observed CO deficiency and peculiar molecular gas distribution in HCG 31 and HCG 92.

Subject headings: galaxies: clusters: individual (HCG 31, HCG 92) — galaxies: interactions — galaxies: evolution — ISM: molecules — infrared: galaxies

1. INTRODUCTION

Study of compact groups of galaxies address several interesting outstanding problems in modern astrophysics. Compact groups represent an important hierarchical link between pairs and clusters of galaxies in structure and evolution. Continuous tidal perturbations in a group environment may promote star formation and mergers, and compact groups seen today may evolve and merge to form large luminous elliptical galaxies (Barnes 1989). Analogous physical processes may also be responsible for the rapid evolution of faint blue galaxies or "chain" galaxies with knotty or disturbed appearances found at moderate redshifts (Cowie, Hu, & Songalia 1995; Glazebrook et al. 1995; Abraham et al. 1996).

In an effort to gauge the impact of continuous tidal interactions on induced star formation and/or morphological and dynamical perturbations within a compact group environment, we have conducted a survey of CO and far-infrared (FIR) emission from a redshift limited complete sample of Hickson compact groups (HCGs; Verdes-Montenegro et al. 1996, hereafter Paper I). Enhanced CO and IR emission is a likely outcome of the gas inflow from the outer disk and the formation of massive stars triggered by tidal disruptions (Braine & Combes 1993; Combes et al. 1994). In Paper I, we reported that some of the HCG galaxies are *deficient* in CO emission for their optical sizes or blue luminosity, while their IR luminosity is normal or slightly enhanced. In order to investigate these peculiar results further, we have conducted a detailed study of CO and IR emission in two CO deficient HCGs, which also show strong evidence for vigorous ongoing tidal interactions.

HCG 31 (NGC 1741, Arp 259, VV 524) is a group of four galaxies in close proximity as identified by Hickson (1982). While the galaxy D is found to be a background object with a discordant redshift, another group member ("G") is later identified (Rubin, Hunter, & Ford 1990; Hickson et al. 1992). Citing complex morphology, small velocity dispersion (<250 km s^{-1}), irregular internal dynamics, and a large common H I envelope (Williams, McMahon, & van Gorkom 1991), Rubin et al. (1990) suggested that HCG 31 is in the process of merging to form a single galaxy. HCG 92 ("Stephan's Quintet") is one of the best known and most studied groups of galaxies because of its ubiquitous tidal features and the controversial presence of a prominent member with discordant redshift (see Sulentic, Pietsch, & Arp 1995, and references therein). A large envelope of H I surrounds HCG 92 (Shostak, Sullivan, & Allen 1984), and diffuse X-ray emission centered on the group is detected with *ROSAT* (Sulentic et al. 1995). In the following sections, the results from high spatial resolution CO observations of HCG 31 and HCG 92 using the Owens Valley millimeter array and the analysis of *IRAS* HIRES maps are presented. We discuss these new results in context of continuous tidal disruptions and resulting effects on the evolution of individual galaxies in the compact group environment.

2. OBSERVATIONS AND RESULTS

2.1. *IRAS HIRES*

We have obtained *IRAS* HIRES images of HCG 31 and HCG 92 in order to trace the distribution of warm dust to complement our CO observations. These HIRES images are resolution enhanced, co-added images of the *IRAS* sky survey data using the Maximum Correlation Method (Aumann, Fowler, & Melnyk 1990). Given sufficient S/N, these HIRES images have 3–5 times improvement in spatial resolution compared with the "full resolution" *IRAS* images. The effective "beam" of the HIRES images depends on the scan

[1] Present address: National Radio Astronomy Observatory, P.O. Box 0, Soccoro, NM 87801; myun@nrao.edu.

coverage in the original survey and the S/N in the data, and the achieved spatial resolutions are about 40″ for 12 and 25 μm bands and 60″–80″ for 60 and 100 μm bands.

The FIR emission in HCG 92 is clearly extended in 60 and 100 μm bands (Fig. 1 [Pl. L5]). The 60 μm emission peaks between HCG 92C and HCG 92B&D and extends toward HCG 92A. The 100 μm emission is also extended and peaks near the group center. All four galaxies are likely contributing to the observed far-infrared emission. The cold dust present in the foreground spiral galaxy HCG 92A (NGC 7320) may contribute significantly at longer wavelengths. HCG 92A has 9 Jy km s^{-1} of integrated CO flux ($M_{\rm H_2} = 10^7\,M_\odot$ if $D = 10$ Mpc; Paper I). The expected 60 μm flux for this gas at 20 K is 330 mJy assuming $L_{FIR}/M_{\rm H_2} = 10\,L_\odot/M_\odot$, and this agrees well with the estimated 60 μm flux of 340 mJy in the HIRES image. The 12 and 25 μm band images are not reliable because they too noisy and their PSFs are also double peaked.

In HCG 31, 12 and 25 μm emission appears to peak on galaxy A, while 60 and 100 μm emission peaks near the overlap region, roughly coincident with the CO emission (Fig. 2 [Pl. L6]). The HIRES images in all four *IRAS* bands are essentially identical to their PSFs (thus not shown). Mimicking the distribution of the extended H I envelope (Williams et al. 1991), the 100 μm emission may be slightly extended toward HCG 31G (Mrk 1090), which is also a faint *IRAS* source (75 and 500 mJy at 25 and 60 μm). The highest S/N is achieved in 60 μm band, and the coincidence of FIR emission with CO emission (see below) suggests that the bulk of warm dust ($T_d \sim 40$ K assuming ν^1 emissivity) is associated with the molecular gas.

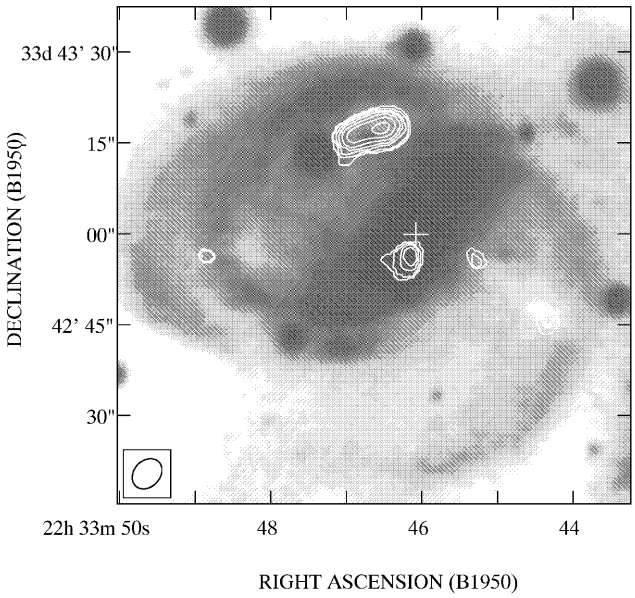

FIG. 3.—Integrated CO (1–0) emission in HCG 92C (NGC 7319) is shown in contours superposed over the 5 m Palomar CCD image (kindly provided by J. Sulentic). The 15% linear contours are shown, and the CO peak correspond to mean H_2 column density of 4.7×10^{21} cm^{-2}. The cross marks the radio position of the nucleus. The primary beam of the OVRO array is 65″ and is centered on R.A. (B1950) = $22^{\rm h}33^{\rm m}46\overset{\rm s}{.}2$ and Decl. (B1950) = +33°43′02″. A single massive molecular complex ($6.2 \times 10^8\,M_\odot$) located 8 kpc north of the nucleus accounts for 72% of the total detected CO emission, while a second massive CO complex is found within 2 kpc of the nucleus. The optical disk shows several prominent dust patches, which are well correlated with the CO features.

2.2. CO

Aperture synthesis CO observations of HCG 31 and HCG 92 were carried out with the Owens Valley Millimeter Array between 1995 September and December. Baselines of 15–200 m E-W and 15–220 m N-S were used, and the synthesized beam was 4.″5 × 6.″0 (PA = −27°) [4.″3 × 5.″5 (PA = −43°)] for HCG 31 [HCG 92] with natural weighting and tapering of the data. There were six 10.4 m diameter telescopes in the array, each equipped with an SIS receiver cooled to 4 K. Typical system temperatures were 300–500 K (SSB). A digital correlator configured with 120 × 4 MHz channels (11.2 km s^{-1}) covered a total velocity range of 1340 km s^{-1}. The nearby quasars 0458−020 and 3C 454.3 were observed at 25 minute intervals to track the phase and short-term instrument gain, and Uranus ($T_B = 120$ K), Neptune ($T_B = 115$ K), 3C 273, and 3C 454.3 were used for the absolute flux calibration. The data were calibrated using the standard Owens Valley array program MMA (Scoville et al. 1992), and DIFMAP (Shepherd, Pearson, & Taylor 1994) and NRAO AIPS were used for mapping and analysis. The uncertainty in flux measurement is about 10%, and the positional accuracy of the resulting maps is better than ∼0.″5.

We observed CO emission in galaxies B (NGC 7318A), C (NGC 7319), and D (NGC 7318B; $D = 86$ Mpc for $H_\circ = 75$ km s^{-1} Mpc^{-1}), and only HCG 92C is detected. The total detected CO flux in HCG 92C is 9.4 Jy km s^{-1} (62% of the flux measured at the NRAO 12 m telescope; Paper I), which corresponds to a total molecular gas mass of $8.6 \times 10^8\,M_\odot$. The interferometer is sensitive to structures smaller than 45″ in size, and some of the missing flux may belong to a larger diffuse structure. Most of the CO features are likely real and physically associated with the galaxy because their velocities correspond to the disk rotation and their positions coincide with prominent dust patches in the disk. The CO distribution is highly asymmetric (see Fig. 3). It is dominated by a single massive complex ($6.2 \times 10^8\,M_\odot$) located 8 kpc north of the nucleus, which is 4.7 kpc in size (unresolved in width) and has average surface mass density of $60\,M_\odot$ pc^{-2}. Another molecular complex found 2 kpc south of the nucleus is unresolved ($d \lesssim 2$ kpc) and has $1.4 \times 10^8\,M_\odot$ of H_2 with mean surface density of $30\,M_\odot$ pc^{-2}. Other faint CO features are unresolved in size and have masses of (2–5) $\times 10^7\,M_\odot$ each. These molecular features have mean surface mass density comparable to the spiral arms of nearby disk galaxies, and the individual complexes have properties similar to the "giant molecular associations" (GMAs) found in M51 and M100 ($M_{\rm H_2} = 10^{7-8}\,M_\odot$, $d = 0.5$–1 kpc; Rand & Kulkarni 1990; Rand 1995). It is also worth noting that no CO emission is detecting in the prominent interacting pair NGC 7318 A and B. Such strongly interacting pairs are generally known to display enhanced CO emission (e.g., Combes et al. 1994).

The CO emission in HCG 31 ($D = 55$ Mpc) is faint. The brightest emission lies in the overlap region between galaxies A and C (Fig. 4), close to the Wolf-Rayet nucleus of galaxy C (Vacca & Conti 1992; Esteban & Peimbert 1995). This also coincides with the peak of FIR emission (see Fig. 2) and probably represents the site of current massive star formation. The CO emitting region is only slightly larger than the synthesized beam (∼2 kpc), with mean surface mass density of $30\,M_\odot$ pc^{-2}. Weak CO emission may also be present within the disks of galaxies A, B, and C. The combined total H_2 mass for galaxies A and C is $2.9 \times 10^8\,M_\odot$, which is 70% of the NRAO

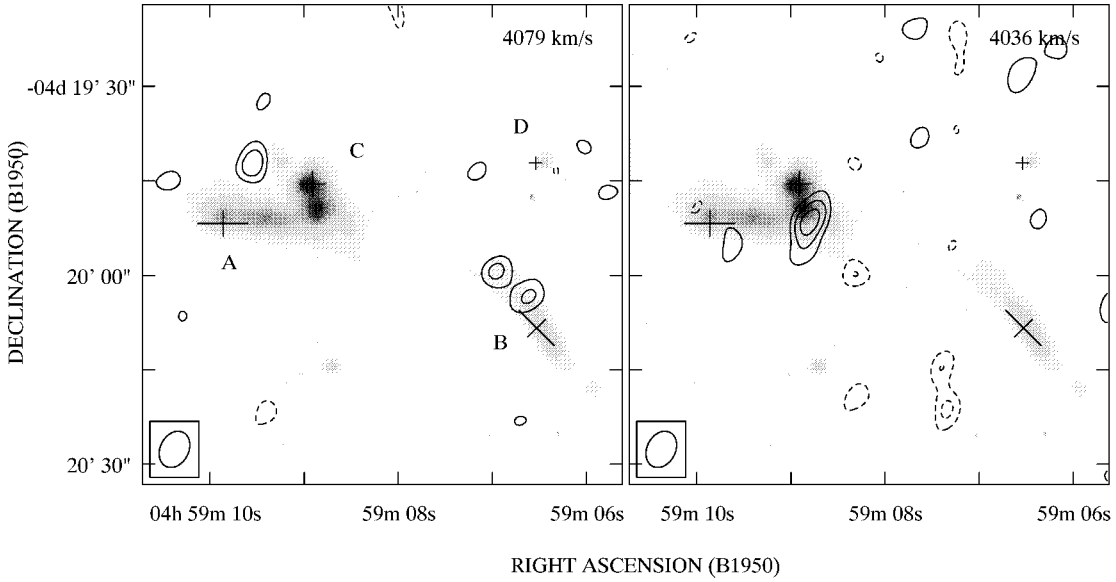

FIG. 4.—43 km s^{-1} channel maps of CO (1–0) emission in HCG 31 are shown superposed over a *V*-band CCD image. The channel center velocities are shown on the upper right corner, and the positions of the four member galaxies given in Hickson et al. (1992) are drawn with crosses. The phase center for these OVRO observations was at R.A. (B1950) = $04^h59^m08\overset{s}{.}2$ and Decl. (B1950) = $-04°19'55''$. The CO emission appears only in these two channels and peaks near the overlap region between HCG 31 A and C. The contours correspond to −3, −2, +2, +3, +4, times the rms noise (11 mJy beam^{-1} or 38 mK) in each channel map.

12 m measurement (Paper I). The H_2 mass of galaxy B may be as large as $10^8\ M_\odot$ if real. All of the detected CO emission occurs within a very narrow range of velocities (4014–4100 km s^{-1}) as in H I and optical (Williams et al. 1991; Rubin et al. 1990).

3. TIDAL DISRUPTIONS AND GAS EXHAUSTION IN COMPACT GROUP ENVIRONMENT

The tidal radius decreases with encounter velocity as $v^{-2/3}$ in the impulse approximation of the tidal disruptions. Small velocity dispersions associated with compact groups (1–2 times typical disk rotation velocity) imply that tidal disruption of individual galaxies is nearly as efficient as for close pairs and 5–10 times more efficient than in clusters. In addition, the galaxy density in HCGs may be as high as in the cores of rich clusters (Hickson et al. 1992), and a net result is that both tidal disruption and gas stripping may be highly efficient in the compact group environment. Nearly every member of HCG 31 and HCG 92 shows signs of recent or ongoing tidal interaction, and the new CO observations also support this tidal disruption scenario.

The molecular gas distribution in HCG 92C is strongly asymmetric, dominated by a single massive complex located 8 kpc away from the nucleus. The observed distribution is highly unusual since CO emission is generally centrally concentrated or found in a symmetric structure like a ring or an arm/bar in galaxies (e.g., Scoville et al. 1991; Kenney, Carlstrom, & Young 1993). HCG 92C shows clear evidence for recent tidal disruptions, and the same tidal disruption responsible for the prominent stellar bar and large tidal tails seen in optical light may also be responsible for the observed CO morphology. The GMAs in the nearby spirals reside along the spiral arms and would last only about the crossing time of a spiral arm ($<10^8$ yr), and the observed molecular gas distribution must also be similarly transient in nature. The brightest CO feature in HCG 31 occurs near the overlap region between galaxies A and C, and enhanced CO emission and associated star formation may be the result of an ongoing collision, similar to that seen in NGC 4038/9 (Stanford et al. 1990).

The total molecular gas detected in HCG 92C ($L_B = 5.5 \times 10^{10}\ L_\odot$) is about 1/3 of the total in our Galaxy, and CO is not detected in HCG 92 B & D ($M_{H_2} < 2 \times 10^8\ M_\odot$ assuming $\Delta V = 300$ km s^{-1}). The total molecular gas detected in the entire HCG 31 group ($L_B = 4.7$ and $0.8 \times 10^{10}\ L_\odot$ for HCG 31AC and B) is only about 1/10 of the gas found in our Galaxy. Such a low molecular gas content for given blue luminosity (or optical size) is seen in several HCG galaxies as reported in Paper I. Their blue luminosity appears normal for their optical sizes, and the far-infrared emission may be slightly enhanced, resulting in M_{H_2}/L_{FIR} ratio more characteristic of slightly perturbed pairs (see Paper I). The median log L_B for the HCG CO survey sample is 10.3, about twice brighter in B compared to the comparison sample of field/isolated galaxies, and low metallicity is not likely account for the low CO emission in most cases.

One possible explanation for the reduced molecular gas among these HCG galaxies is tidal stripping. Sulentic et al. (1995) have reported $7 \times 10^9\ M_\odot$ of diffuse X-ray gas centered on HCG 92 with solar metallicity and cooling time of 10^8 years and suggested tidally stripped gas from individual galaxies as a possible origin. The distribution of the extended X-ray emission and *IRAS* 60 μm emission (Fig. 1) is remarkably similar and may indicate presence of warm dust in this intragroup gas. Presence of such X-ray emitting intragroup gas has been suggested as a test of physical reality of compact groups (Ostriker, Lubin, & Herquist 1995), and diffuse, extended gas has also been detected in several other groups (Pildis, Bregman, & Evrard 1995; Saracco & Ciliegi 1995; Mulchaey et al. 1996). A strong correlation between the detection of an X-ray emitting intragroup medium and the percentage of early type (E and S0) galaxies suggests a possible evolutionary scenario in which the intragroup medium is enriched by the stripped ISM of individual galaxies by the dynamical evolution of the groups via tidal interactions and mergers.

Another potentially significant mechanism for the molecular gas depletion among HCG galaxies is star formation. In demonstrating the gas inflow and triggering of starburst during

a merger of two disk galaxies, Mihos & Hernquist (1996) find that some 50%–75% of the total gas is converted to stars. And more importantly, they find that *the majority of gas conversion occurs prior to the actual coalescence of two galaxies* unless the gas inflow is regulated (e.g., by a massive bulge; see their Fig. 15). Because this enhanced star formation is the direct result of increased gas density by tidally driven gas compression, a similar mechanism should also operate in nonmerging integrations, given that tidal disruptions are sufficiently strong. The unique compact group environment in which tidal disruptions may be both continuous and strong (see above) may promote a higher sustained rate of star formation and thus fast exhaustion of the gas supply. In Paper I, we reported enhanced FIR luminosity to molecular gas mass ratio for the HCG galaxies—about 3 times larger than the comparison sample and more characteristic of interacting pairs—in support of tidally induced star formation among the HCG galaxies.

In summary, the observed CO deficiency and peculiar molecular gas distributions in HCG 31 and HCG 92 can be explained by the scenario that these galaxies are subject to continuous tidal disruptions. Both tidally induced star formations and tidal stripping may be at work, resulting in a reduced current molecular gas reserve.

The authors thank J. Hibbard, C. Mihos, and J. Sulentic for useful discussions. We also thank J. Mazzarella for his discussion on the limitations of *IRAS* data products. This research is supported in part by NSF grant AST 93-14079. L. V.-M., J. P., and A. O. are partially supported by DGICYT (Spain) grant PB93-0159 and Junta de Andalucía (Spain).

REFERENCES

Abraham, R. G., Tanvir, N. R., Santiago, B. X., Ellis, R. S., Glazebrook, K., & van den Bergh, S. 1996, MNRAS, 279, L47
Aumann, H. H., Fowler, J. W., & Melnyk, M. 1990, AJ, 99, 1674
Barnes, J. E. 1989, Nature, 338, 123
Braine, J., & Combes, F. 1993, A&A, 269, 7
Combes, F., Prugniel, P., Rampazzo, R., & Sulentic, J. W. 1994, A&A, 281, 725
Cowie, L. L., Hu, E. M., & Songaila, A. 1995, AJ, 110, 1576
Esteban, C., & Peimbert, M. 1995, A&A, 300, 78
Glazebrook, K., Ellis, R., Santiago, B., & Griffiths, R. 1995, MNRAS, 275, L19
Hickson, P. 1982, ApJ, 255, 382
Hickson, P., de Oliveira, C. M., Huchra, J. P., & Palumbo, G. G. C. 1992, ApJ, 399, 353
Kenney, J. D. P., Carlstrom, J. E., & Young, J. S. 1993, ApJ, 418, 687
Lasker, B. M., et al. 1990, AJ, 99, 2019
Mihos, J. C., & Hernquist, L. 1996, ApJ, 464, 641
Mulchaey, J. S., Davis, D. S., Mushotzky, R. F., & Burstein, D. 1996, ApJ, 456, 80
Ostriker, J. P., Lubin, L. M., & Hernquist, L. 1995, ApJ, 444, L61
Pildis, R. A., Bregman, J. N., & Evrard, A. E. 1995, ApJ, 443, 514
Rand, R. J 1995, AJ, 109, 2444
Rand, R. J., & Kulkarni, S. R. 1990, ApJ, 349, L43
Rubin, V. C., Hunter, D. A., & Ford, W. K. 1990, ApJ, 365, 86
Saracco, P., & Ciliegi, P. 1995, A&A, 301, 348
Scoville, N. Z., Carlstrom, J. C., Chandler, C. J., Phillips, J. A., Scott, S. L., Tilanus, R. P., & Wang, Z. 1992, PASP, 105, 1482
Scoville, N. Z., Sargent, A. I., Sanders, D. B., & Soifer, B. T. 1991, ApJ, 366, L5
Shepherd, M. C., Pearson, T. J., & Taylor, G. B. 1994, BAAS, 26, 987
Shostak, G. S., Sullivan, W. T., & Allen, R. J. 1984, A&A, 139, 15
Stanford, S. A., Sargent, A. I., Sanders, D. B., & Scoville, N. Z. 1990, ApJ, 349, 492
Sulentic, J. W., Pietsch, W., & Arp, H. 1995, A&A, 298, 420
Vacca, W. D., & Conti, P. S. 1992, ApJ, 401, 543
Verdes-Montenegro et al. 1996, A&A, submitted (Paper I)
Williams, B. A., McMahon, P. M., & van Gorkom, J. H. 1991, AJ, 101, 1957

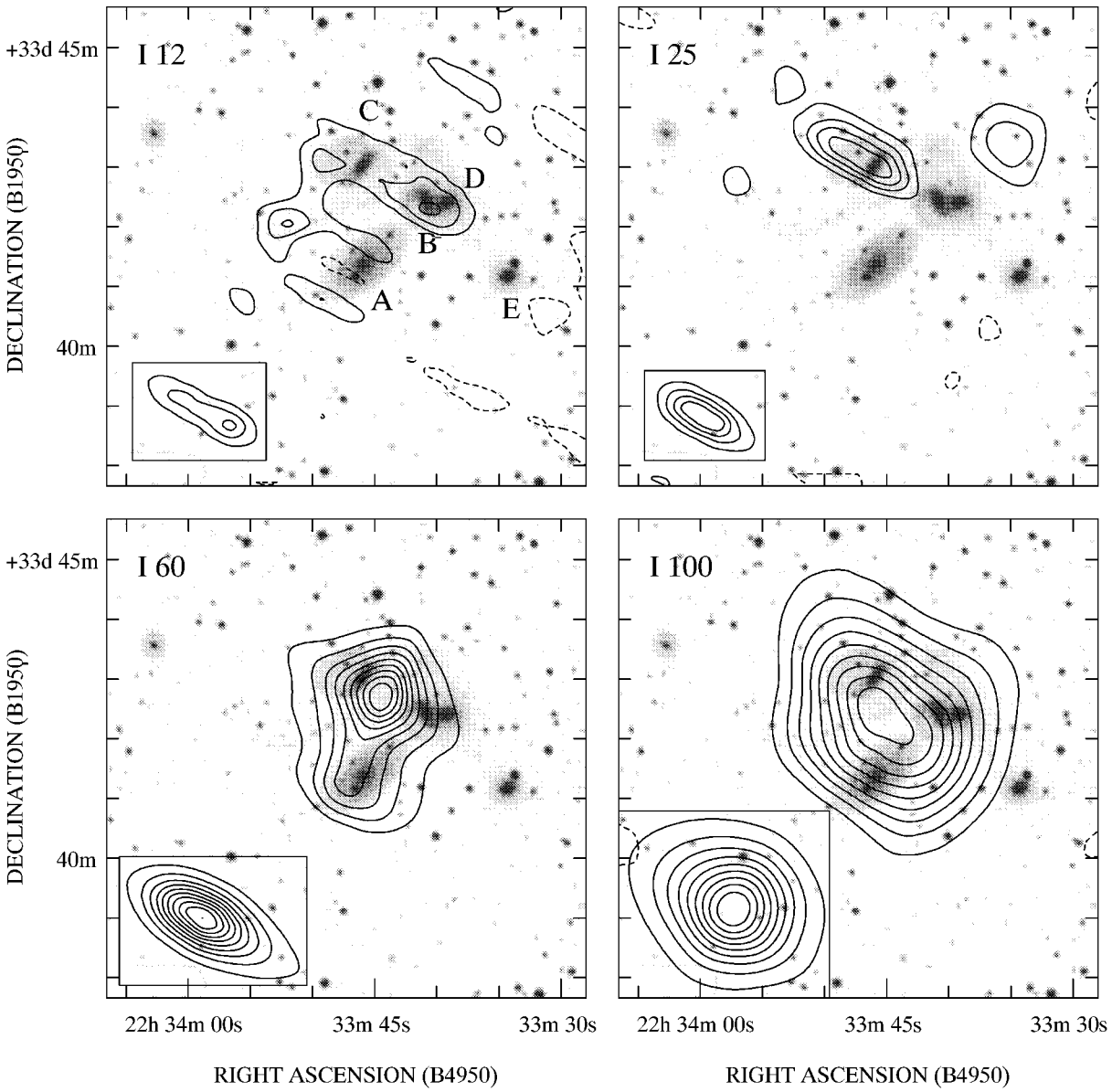

FIG. 1.—HIRES maps of HCG 92 in four *IRAS* bands are shown superposed on the Digitized Sky Survey (DSS) E plate image (see Lasker et al. 1990). The HIRES PSFs (determined from the *IRAS* scan directions and sensitivity) are shown on the bottom left corner, and the *IRAS* emission appears to originate from at least three of the five group members identified in the figure. Both 60 and 100 μm emission are clearly extended and are centered among the galaxies A, B, C, and D. The contours drawn are linear increments of 10% of the peak brightness for the 60 and 100 μm maps. The contours for the 12 and 25 μm maps are in increments of 30% and 20% of the peak, respectively.

YUN et al. (see 475, L22)

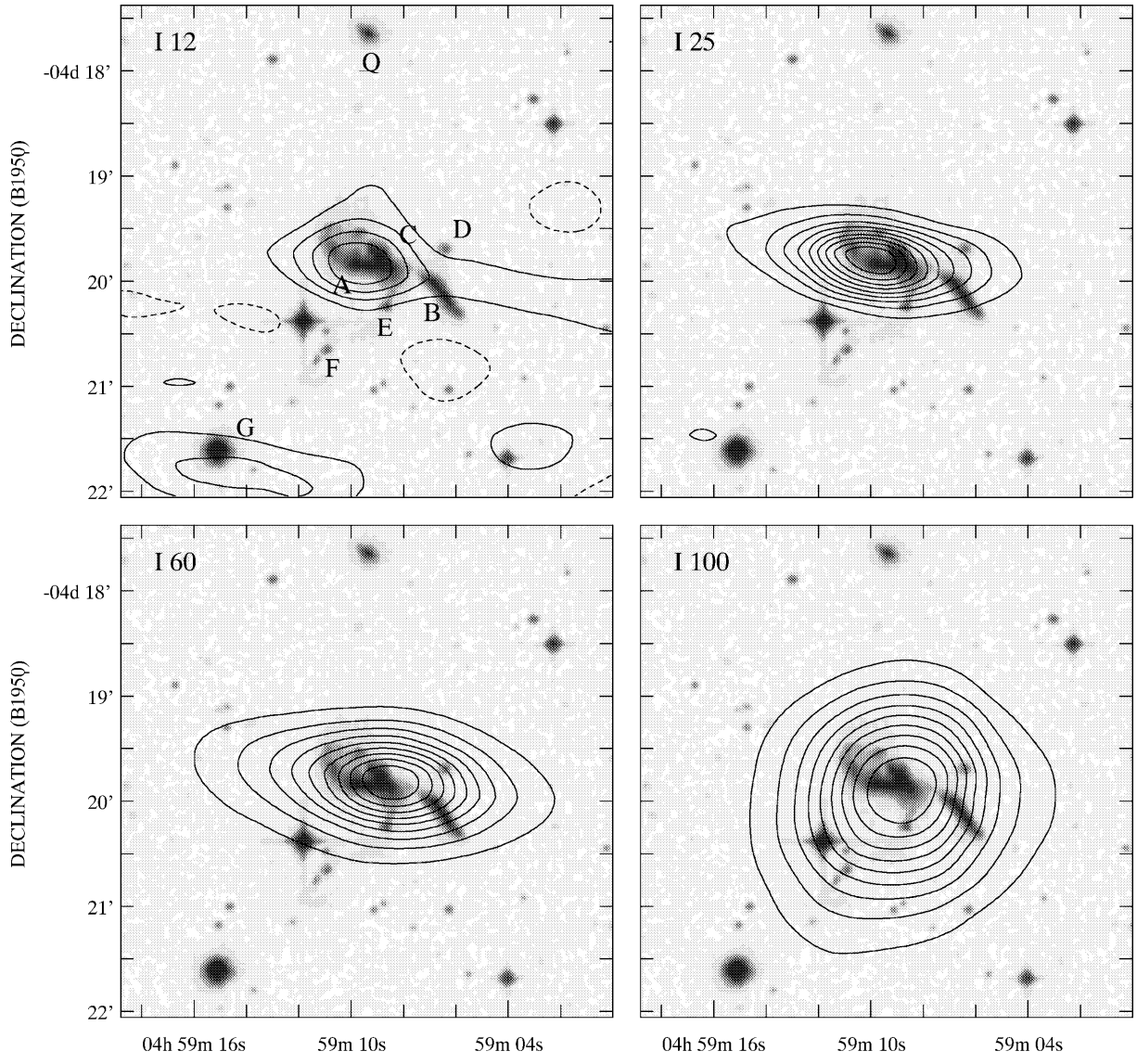

FIG. 2.—HIRES maps of HCG 31 in four *IRAS* bands are shown superposed on the Digitized Sky Survey (DSS) E plate image (see Lasker et al. 1990). The four main group members as well as other objects found by Rubin et al. (1990) are identified in the figure. The 12 and 25 μm emission appears to peak on galaxy A, while the 60 and 100 μm emission peaks occur near the overlap region, coincident with the CO emission (see Fig. 4). The *IRAS* source appears unresolved in all four bands based on the comparison with the PSF. The 100 μm emission may be slightly extended toward HCG 31G (Mrk 1090), which is also a faint *IRAS* source. The contours shown are linear increments of 10% of the peak brightness except at 12 μm (20%). The 12 and 25 μm emission may indicate the presence of hot dust around the nucleus of HCG 31A, but S/N is low.

YUN et al. (see 475, L22)